JÜLICH
FORSCHUNGSZENTRUM

Towards 3D GPR full-waveform inversion

Near surface FWI workshop Zürich

Amirpasha Mozaffari ❖, Anja Klotzsche ❖, Guowei He ❖, Antonis Giannopoulos ✢, Craig Warren ✢, Harry Vereecken ❖, Jan van der Kruk ❖

❖Forschungszentrum Jülich, ✢University of Edinburgh

2D-Full Wave Inversion (FWI)

Data
Pre – processing

Source
estimation

2D Full-wave
form
inversion

3D to 2D Transformation

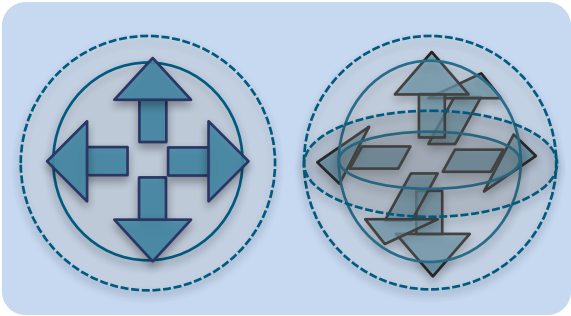

Bleistein Assumptions
- Far-Field approximation
- Slowly varying medium properties

Bleistein transformation

Transforming the 3D geometrical spreading to 2D & source dimension (Bleistein 1986)

$$\hat{E}^{2D} = \hat{E}^{3D}\sqrt{\frac{2\pi T}{-i\omega\varepsilon^{mean}\mu_0}}$$

(Ernst et al. 2007)

Measured & 2D transformed data

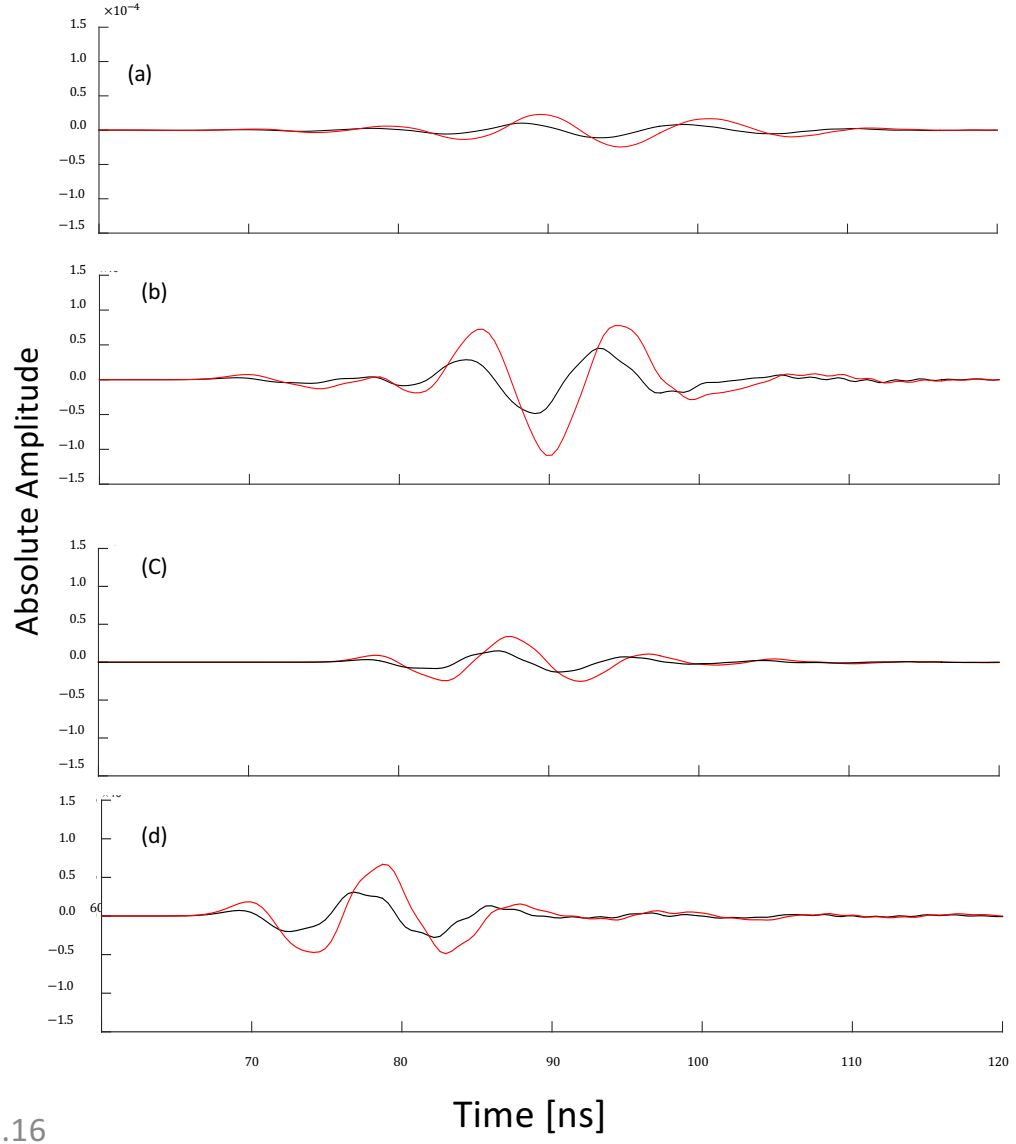

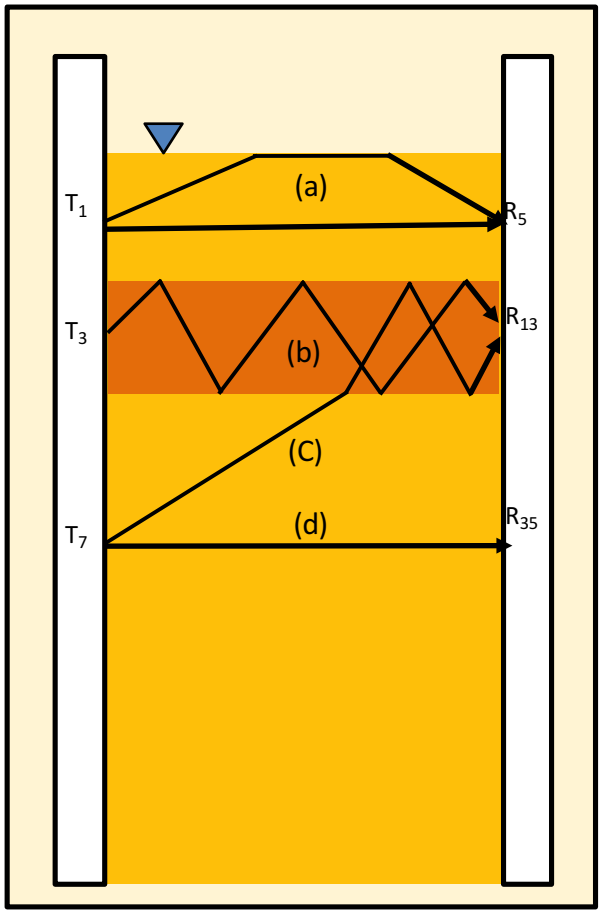

Original observed trace (3D)

Bleistein transformed trace (2D)

3D-FWI Benefits

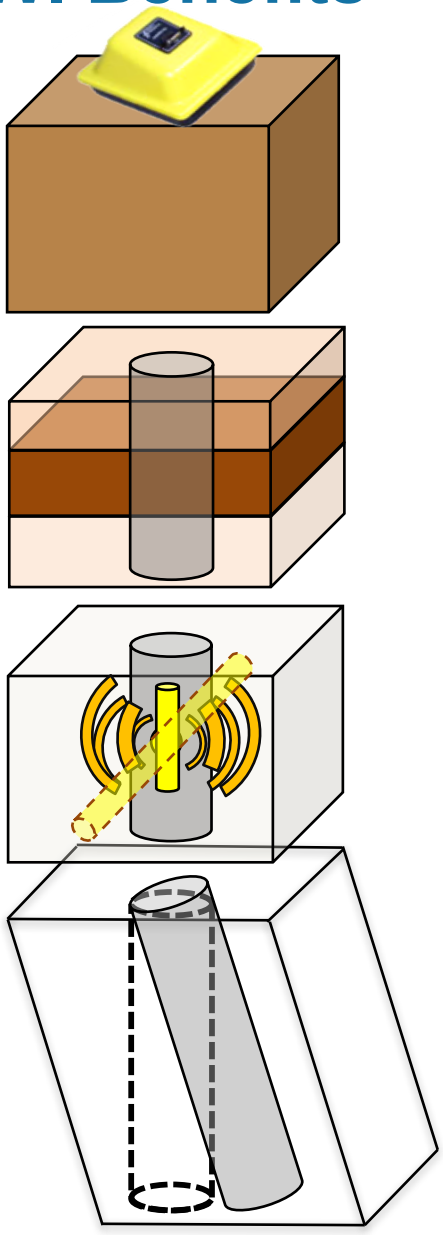

On ground GPR FWI

Removing transformation will cancel out the necessity of the far-field assumption

High contrast layer (late time arrival)

- More reliable reconstruction of the high contrast layers by canceling out the data transformation

Antenna Modeling

More realistic model by replacing line source (2D) with point source **+ finite length antenna possibility**

Realistic Borehole modeling

Physical presence of the borehole and possible deviation of it, could modeled in more detail

2.5D-Full Wave Inversion (FWI)

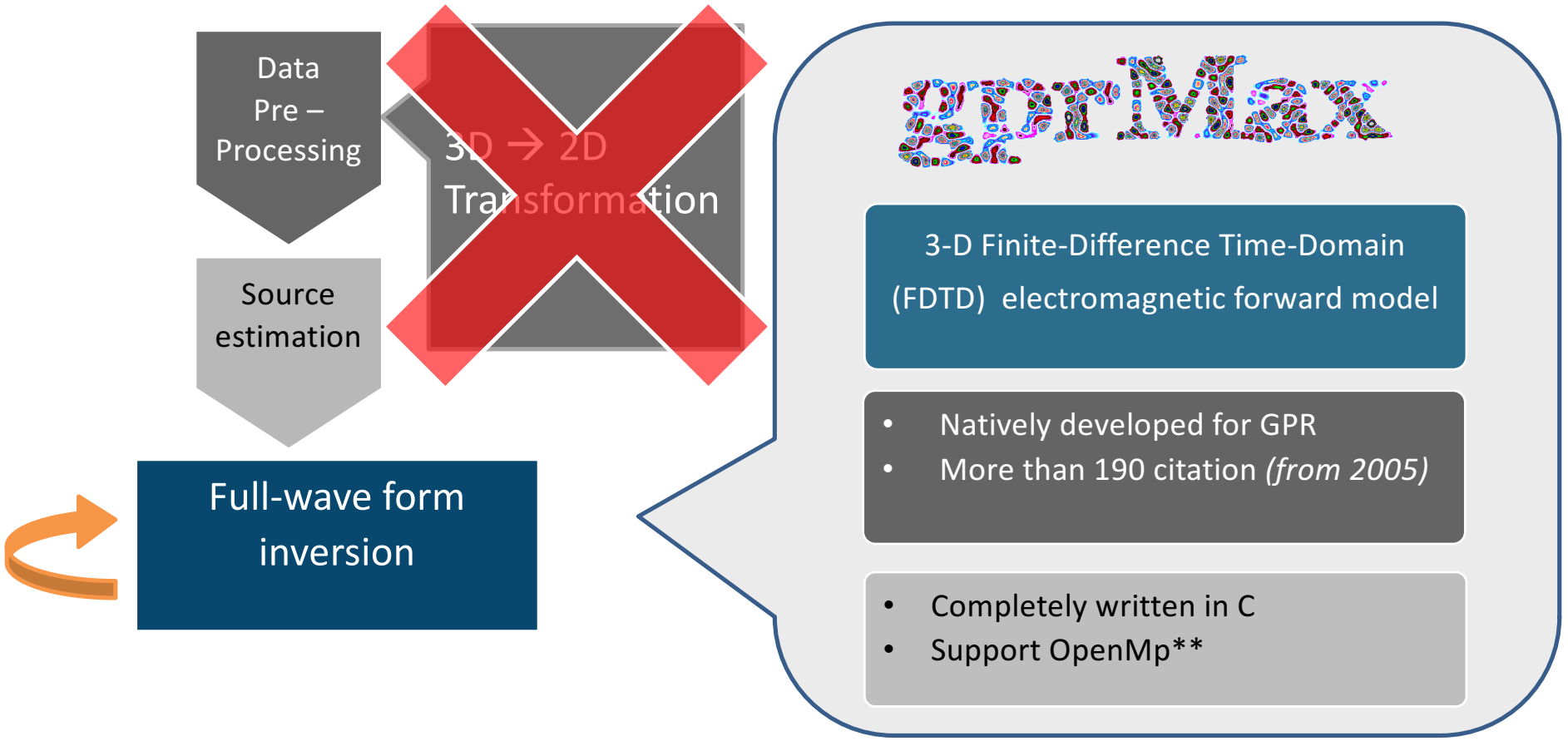

gprMax* is available for free on www.gprmax.com

OpenMp** (Open Multi-Processing): API that support multi-platform shared memory multiprocessing programing.

2.5-D FWI by using 3D forward model

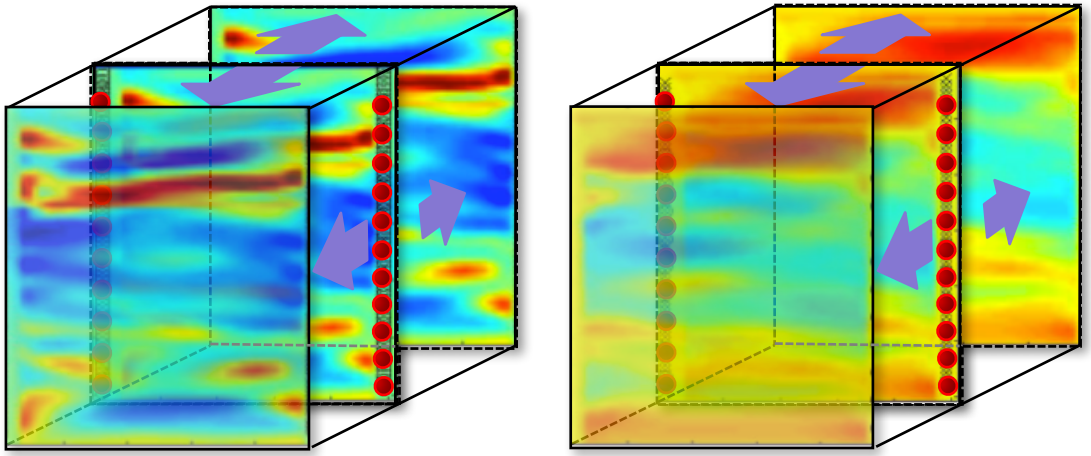

Extend models in 3D

Calculate the fields in 3D

Calculate inversion parameters in one plane

Update the ε and σ models one plane

Permittivity model (left) and conductivity model (right)

Realistic synthetic model

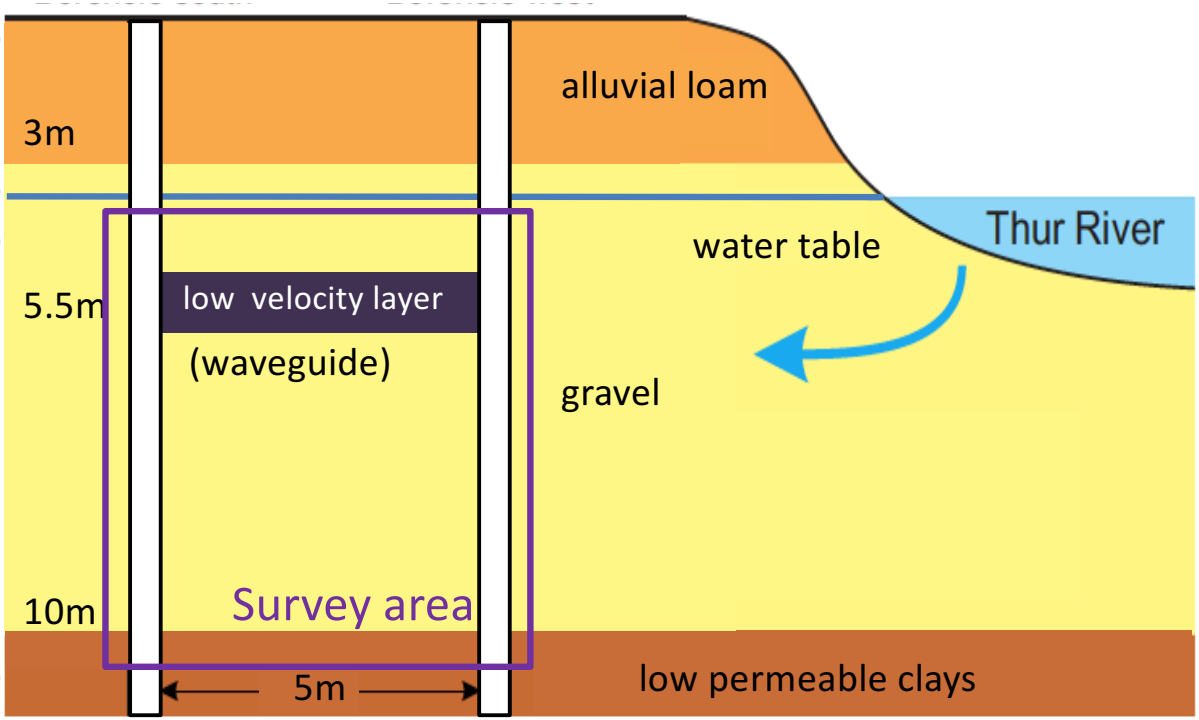

Input model

- Complex structure and presence of the High contrast layer (HCL)
- Well studied dataset (e. g. Klotzsche 2012)

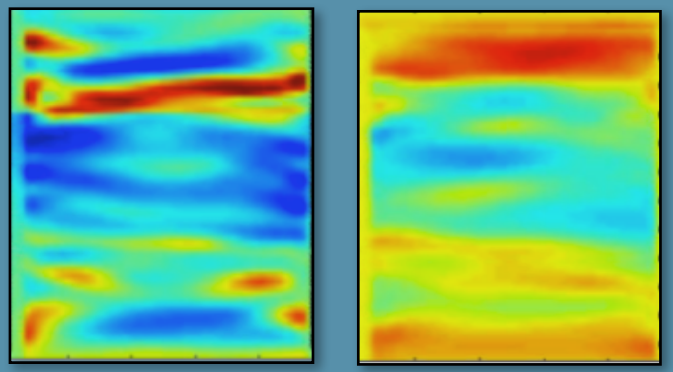

Permittivity Conductivity

Widen test site near the River Thur, Switzerland (Figure adopted from Klotzsche et al. 2012)

2.5D FWI (Improved RBSM)

Homogenous conductivity starting model

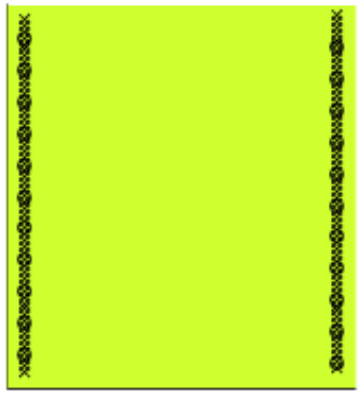

Improved permittivity ray-based inversion results starting model

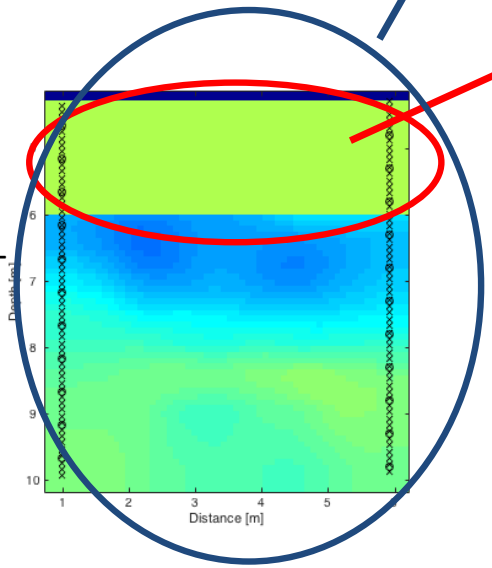

Permittivity ray-based inversion result + Homogenous Conductivity model

↓

Poor ray-coverage near to water table

↓

Improved permittivity model

↓

Overlap the model and observed data within half the dominant pulse period for both **2D** and **2.5D FWI**

2.5 D FWI is more sensitive to starting model

2.5D FWI (Improved RBSM)

Realistic synthetic model

Known source wavelet ✓

Known True model ✓

Error Model

$$\xi(m_{cal})_{\sigma,\varepsilon} = 100\times\left(\frac{m_{cal}-m_{true}}{m_{true}}\right)_{\sigma,\varepsilon}$$

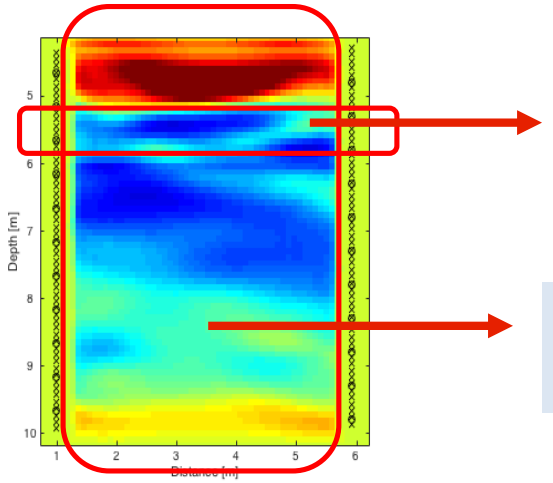

2.5D FWI (Improved RBSM)

2D

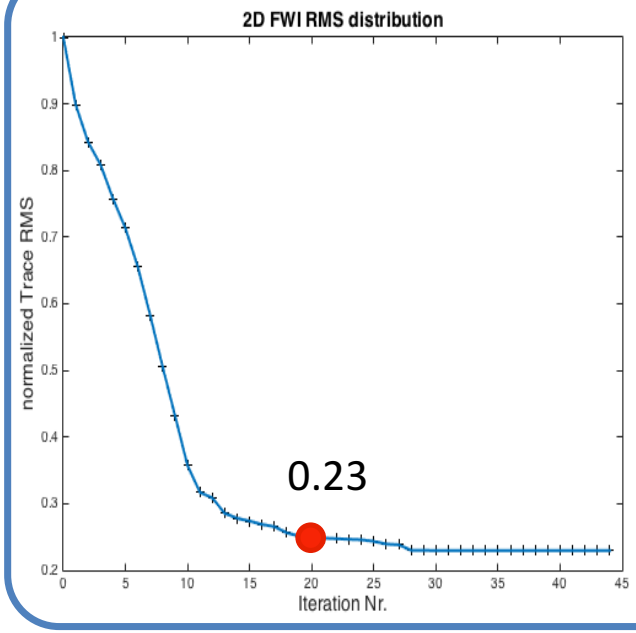

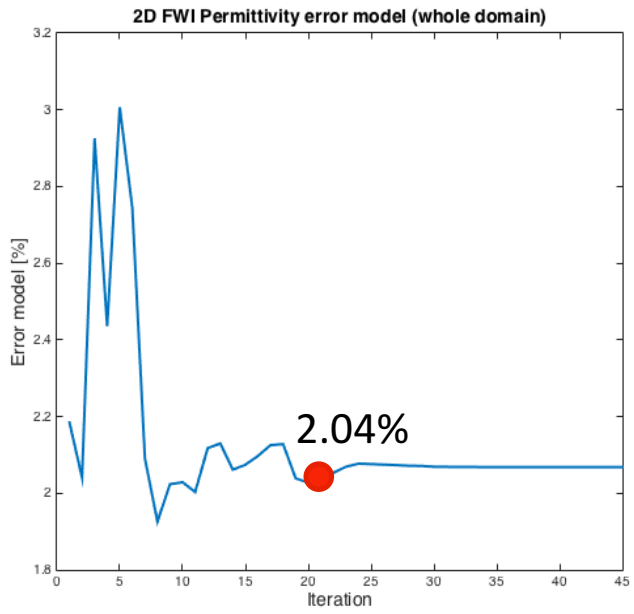

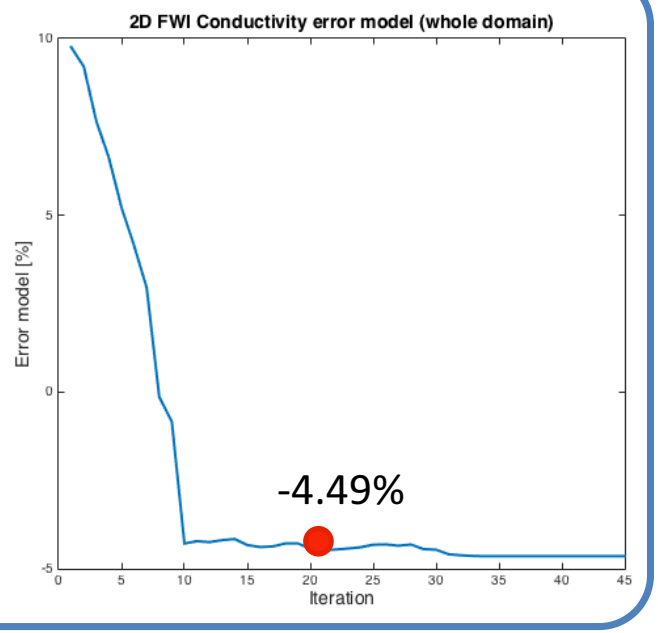

2.5D

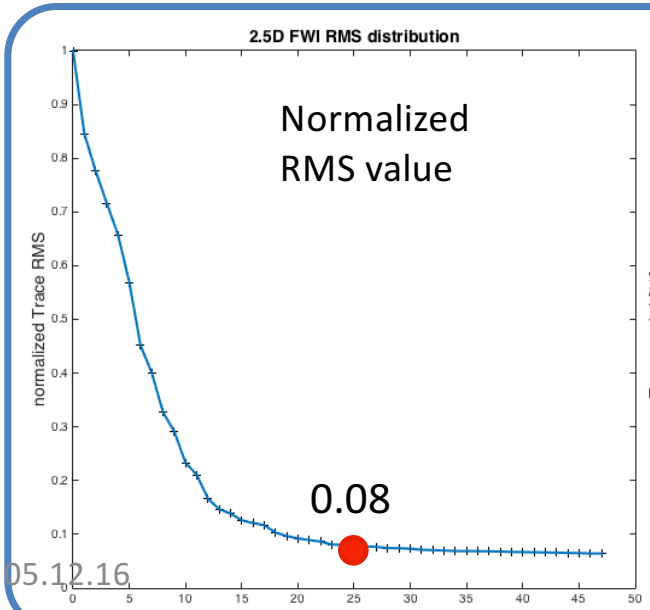

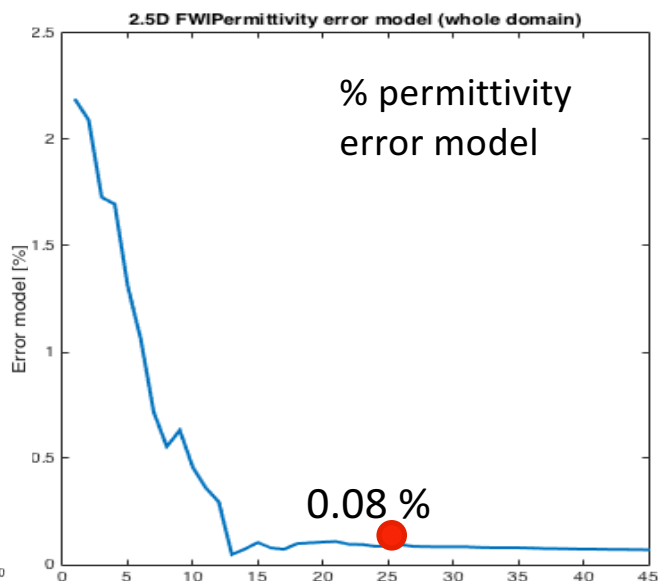

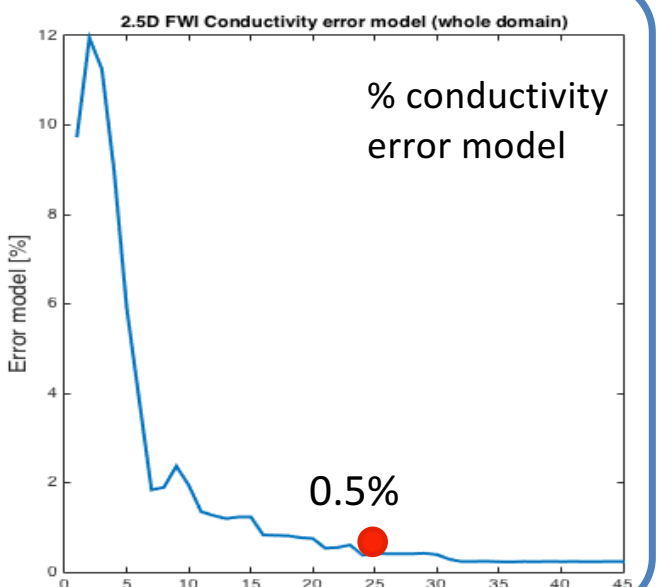

2.5D Error models

Horizontal permittivity error model

Horizontal conductivity error model

2D

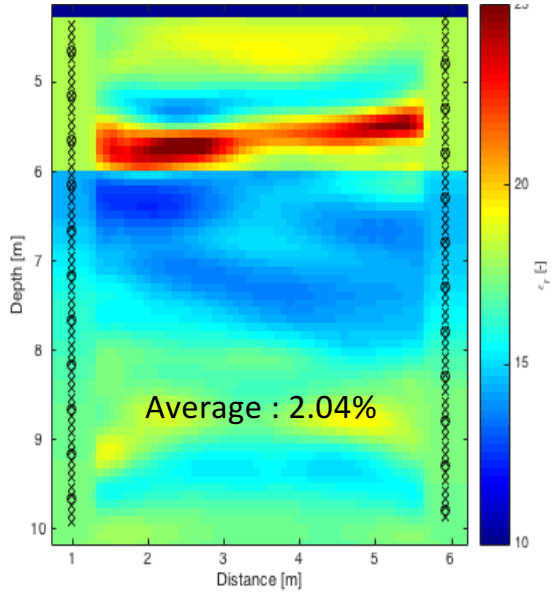

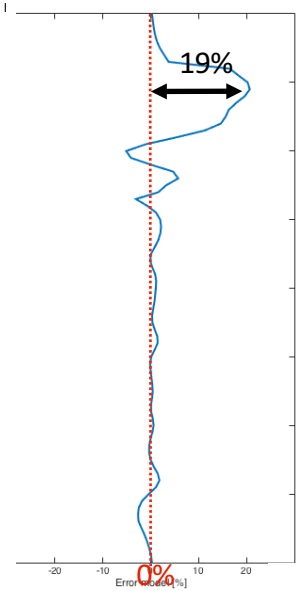

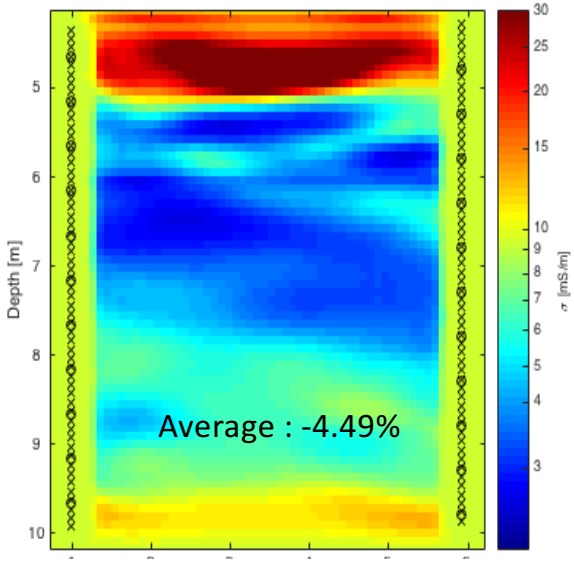

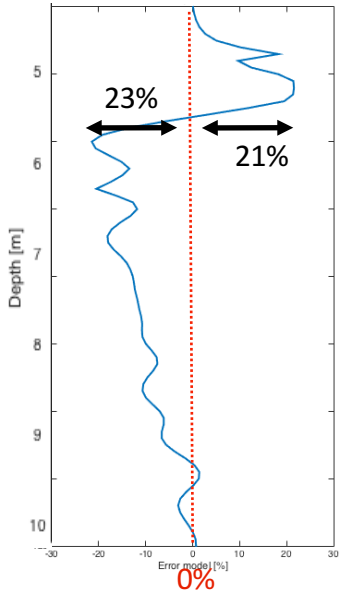

2.5D

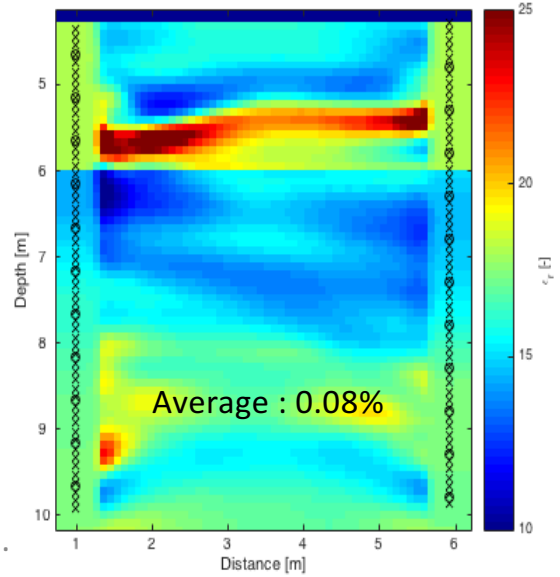

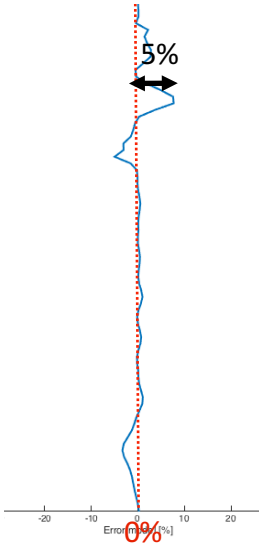

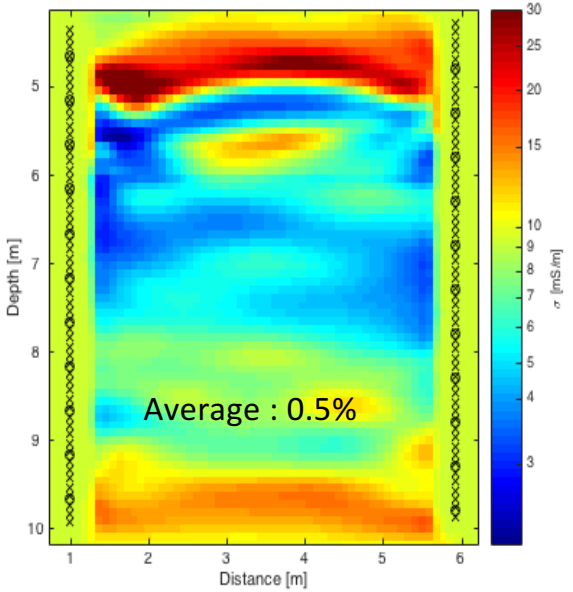

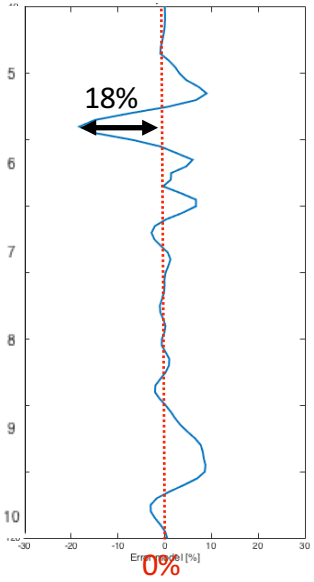

2.5D FWI (Improved RBSM)

2D FWI
30 iterations (48 core)
6 m. 43 s. → 0.16 Core-h/ it

2.5D FWI
30 Iteration (96 core)
29 h. 54 m. → 95.68 Core-h/it

≈ 600x higher computation intensity

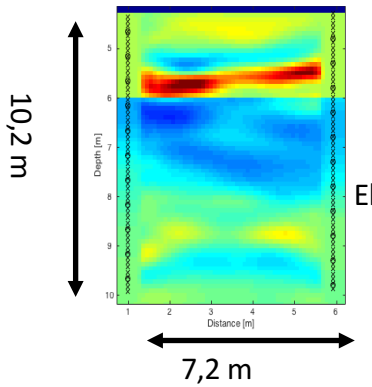

Element size : 0,09m

Elements numbers : 9600

2x Intel Xeon E5-2680 CPU/nod

2 x 12 cores, 2.5 GHz

2.5-D FWI (Intermediate SM)

Improved Ray-based inversion result (RBSM) (Klotzsche et al.2012)

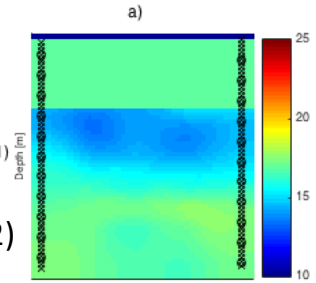

2D FWI

Intermediate Starting model (ISM)

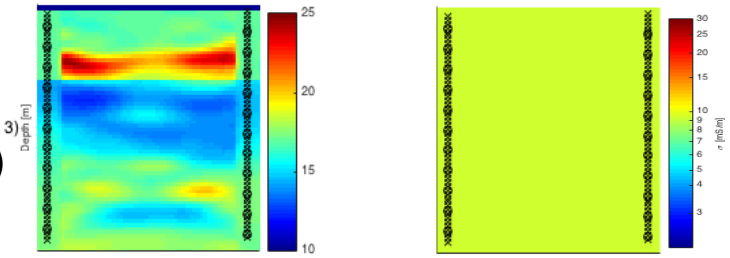

2.5D FWI

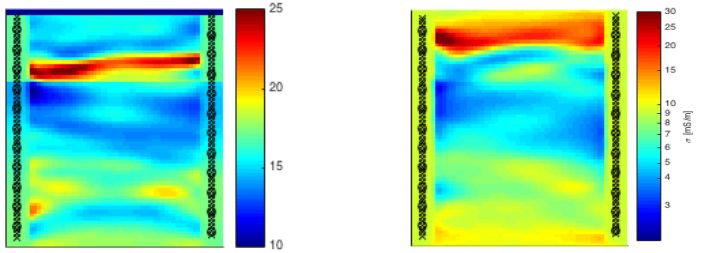

Starting model : based on ray-Based inversion for 2D FWI

2-D FWI intermediate permittivity model is used as 2.5-D FWI starting model

2.5D FWI

Results of the 2.5-D FWI

Outlook

New generation gprMax is enable to model antenna design and includes several commercial antenna model

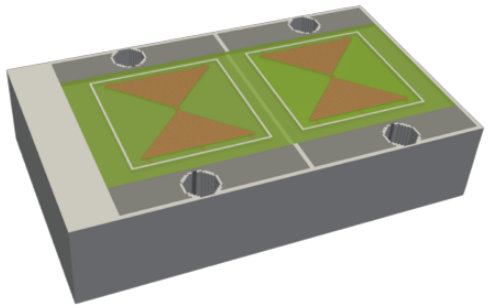

Mala Geoscience 1.2 GHz antenna included in new gprMax

FWI

Finite Antenna Length Implementation

More realistic model by replacing the point source antenna with finite length antenna in forwarding model that adopted from gprMax

Geoscanners BA 1000 antenna

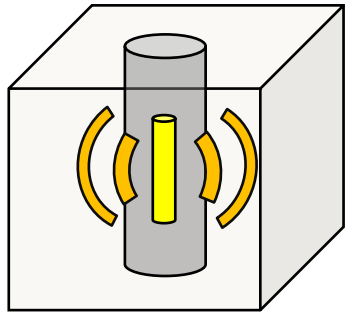

Conclusion

we have extended the 2D FWI to 2,5D by replacing 2D FDT with 3D gprMax FDTD forward model

2.5 FWI is more sensitive to starting model than 2D FWI

2.5D FWI showed better results for permittivity and conductivity in compare to 2D FWI for realistic synthetic models

Sufficient detailed starting model for 2.5D FWI is obtained by using a low number iteration result of 2D FW.

JÜLICH
FORSCHUNGSZENTRUM

Thank you for your attention!

References

Auer, L., Nuber, A. M., Greenhalgh, S. A., Maurer, H., & Marelli, S. (2013). A critical appraisal of asymptotic 3D-to-2D data transformation in full-waveform seismic crosshole tomography. *Geophysics*, *78*(6)

Busch, S., van der Kruk, J., Bikowski, J., & Vereecken, H. (2012). Quantitative conductivity and permittivity estimation using full-waveform inversion of on-ground GPR data. *Geophysics*,

Ernst, J. R., Member, S., Maurer, H., Green, A. G., & Holliger, K. (2007,a). Full-Waveform Inversion of Crosshole Radar Data Based on 2-D Finite-Difference Time-Domain Solutions of Maxwell ' s Equations. *Ieee*, *45*(9), 2807–2828.

Ernst, J. R., Green, A. G., Maurer, H., & Holliger, K. (2007,b). Application of a new 2D time-domain full-waveform inversion scheme to crosshole radar data. *Geophysics*, *72*(5), J53.

Giannopoulos, A. (2005). *GprMax2D/3D User's Manual*. Retrieved from gprmax.org

Meles, G. A., Van Der Kruk, J., Greenhalgh, S. a., Ernst, J. R., Maurer, H., & Green, A. G. (2010). A new vector waveform inversion algorithm for simultaneous updating of conductivity and permittivity parameters from combination crosshole/borehole-to- surface GPR data. *IEEE Transactions on Geoscience and Remote Sensing*, *48*(9), 3391–3407.

Klotzsche, A., & Kruk, J. van der. (2014). Detection of spatially limited high-porosity layers using crosshole GPR signal analysis and full-waveform inversion. *Water Resources …*,.Received

Klotzsche, A., Kruk, J. Van Der, Mozaffari, A., Gueting, N., & Vereecken, H. (2015). Crosshole GPR full-waveform inversion and waveguide amplitude analysis : Recent developments and new challenges, 1–6.

Klotzsche, A., van der Kruk, J., Meles, G. a., Doetsch, J., Maurer, H., & Linde, N. (2010). Full-waveform inversion of cross-hole ground-penetrating radar data to characterize a gravel aquifer close to the Thur River, Switzerland. *Near Surface Geophysics*, *8*(1750), 635–649

Klotzsche, A., van der Kruk, J., Meles, G., & Vereecken, H. (2012). Crosshole GPR full-waveform inversion of waveguides acting as preferential flow paths within aquifer systems. *Geophysics*, *77*(4), H57–H62.

Kruk, J. van der, Gueting, N., Klotzsche, A., G. He, S. R., C. Hebel, X. Y., Weihermüller, L., … Vereecken, H. (n.d.). Quantitative multi-layer electromagnetic induction inversion and full-waveform inversion of crosshole ground penetrating radar data. *Journal of Earth Science*. In press

Lavoué, F., Brossier, R., Garambois, S., & Virieux, J. (2012). Permittivity and Conductivity Reconstruction by Full Waveform Inversion of GPR Data using the L- BFGS-B Algorithm. In *Near surface 2012* (pp. 3–5).

Lavoué, F., Brossier, R., Métivier, L., Garambois, S., & Virieux, J. (2014). Two-dimensional permittivity and conductivity imaging by full waveform inversion of multioffset GPR data: A frequency-domain quasi-Newton approach. *Geophysical Journal International*, *197*(1), 248–268.

Van Vorst, D. G., Yedlin, M. J., Virieux, J., & Krebes, E. S. (2014). Three-dimensional to two-dimensional data conversion for electromagnetic wave propagation using an acoustic transfer function: application to cross-hole GPR data. *Geophysical Journal International*, *198*(1), 474–483. http://doi.org/10.1093/gji/ggu111

Yang, X., Klotzsche, A., Meles, G., Vereecken, H., & Van Der Kruk, J. (2013). Improvements in crosshole GPR full-waveform inversion and application on data measured at the Boise Hydrogeophysics Research Site. *Journal of Applied Geophysics*.